Available online at www.sciencedirect.com
SCIENCE DIRECT®
Computers and Chemical Engineering 28 (2004) 2021–2036
Computers & Chemical Engineering
www.elsevier.com/locate/compchemeng

Nonequilibrium modeling of three-phase distillation

A. Higler [a], R. Chande [b], R. Taylor [a,b,*], R. Baur [c], R. Krishna [c]

[a] *Department of Science and Technology, Universiteit Twente, Postbus 217, 7500 AE Enschede, The Netherlands*
[b] *Department of Chemical Engineering, Clarkson University, Box 5705, Potsdam, NY 13699, USA*
[c] *Department of Chemical Engineering, University of Amsterdam, Nieuwe Achtergracht 166, 1018 WV Amsterdam, The Netherlands*

Received 12 August 2003; received in revised form 13 April 2004; accepted 13 April 2004

Abstract

A nonequilibrium (NEQ) model for a complete three-phase distillation in tray columns is described. The model consists of a set of mass and energy balances for each of the three possible phases present. Mass and heat transfer between these phases is modeled using the Maxwell–Stefan equations. Equilibrium is only assumed at the phase boundary between two phases. The equilibrium stage model is a special case of the general model.

The method of solving the NEQ model equations described here consists of first solving the equilibrium two phase model, using this solution to obtain a converged solution for the equilibrium three-phase problem by means of a differential arc length continuation method, and subsequently using this as a starting guess for the nonequilibrium three-phase model with Newton's method. Incorporated into the algorithm model is a liquid phase stability check and phase split calculation to evaluate the thermodynamic stability of all liquid phases present in the distillation column each iteration.

We have found that the component Murphree efficiencies tend to be lower and more highly variable in the two-liquid phase region than they are in the single liquid region. There may be a jump discontinuity in component efficiencies as we move from homogeneous to heterogeneous liquid phase regions of composition space. EQ models modified by efficiency factors should not, in general, be used for the simulation of three-phase distillation processes. NEQ models should be preferred in general.

Keywords: Three-phase distillation; Nonequilibrium model; Rate-based model; Maxwell–Stefan

1. Introduction

Chemical engineers have been solving distillation problems using the *equilibrium* (EQ) *stage model* since Sorel first used the model for the distillation of alcohol over 100 years ago. Since the late 1950s chemical engineers have been solving the EQ model equations by computer. Indeed, from the late 1950s to the early 1990s hardly a year passed without the publication of at least one (and usually many more than one) new algorithm for solving these equations (Seader, 1985). One could even make a case that it was the EQ model that brought computing into chemical engineering in the first place.

Real distillation processes, however, nearly always operate away from equilibrium. In recent years it has become possible to simulate distillation and absorption as the mass transfer rate-based operations that really they are using what have become known as *nonequilibrium* (NEQ) or *rate-based* models (Taylor, Krishna, & Kooijman, 2003).

It is the purpose of this paper to discuss the NEQ modeling and computer simulation of three-phase distillation systems. The computer simulation of distillation processes, whether done using EQ or NEQ models, requires us to address the following concerns.

- Formulation of the model equations.
- Physical property calculations.
- Degrees of freedom analysis.
- Solving large linear and strongly nonlinear systems of equations.

These are, in fact, the topics discussed in the influential monograph *Process Flowsheeting* by Westerberg,

* Corresponding author. Tel.: +1-315-268-6652; fax: +1-315-268-6654.
E-mail address: taylor@clarkson.edu (R. Taylor).

0098-1354/$ – see front matter © 2004 Published by Elsevier Ltd.
doi:10.1016/j.compchemeng.2004.04.008

Nomenclature

a_v	interfacial area per volume of vapor (m^{-1})
a_j^{LL}	interfacial area between the two liquid phases on stage j (m^2)
$a_j^{VL'}$	interfacial area between vapor and liquid phase 1 on stage j (m^2)
$a_j^{VL''}$	interfacial area between vapor and liquid phase 2 on stage j (m^2)
c	number of components
c_t	total concentration ($mol\,m^{-3}$)
d_b	bubble diameter (m)
$\mathcal{D}$	Maxwell–Stefan diffusion coefficient ($m^2\,s^{-1}$)
E_j	energy transfer rate on stage j ($J\,s^{-1}$)
E^V	vaporization efficiency
$f_{i,j}$	molar feed stream of component i to stage j ($mol\,s^{-1}$)
F_j	molar feed stream to stage j ($mol\,s^{-1}$)
Fo	Fourier number
g	Gravitation constant ($m\,s^{-2}$)
h_f	Froth height (m)
h_j	heat transfer coefficient ($J\,m^{-2}\,K^{-1}\,s^{-1}$)
H	enthalpy ($J\,mol^{-1}$)
$\bar{H}_{i,j}$	partial molar enthalpy of component i on stage j ($J\,mol^{-1}$)
$K_{i,j}$	equilibrium constant of component i on stage j
L'_j	molar liquid flow rate of phase 1 from stage j ($mol\,s^{-1}$)
L''_j	molar liquid flow rate of phase 2 from stage j ($mol\,s^{-1}$)
$\mathsf{N}_{i,j}$	mass transfer rate of component i on stage j ($mol\,s^{-1}$)
P_j	pressure on stage j (Pa)
Q_j	heat duty on stage j ($J\,s^{-1}$)
R	gas constant ($J\,mol^{-1}\,K^{-1}$)
Sh	Sherwood number
t	homotopy parameter
T	temperature (K)
v_b	bubble rise velocity ($m\,s^{-1}$)
V_j	molar vapor flow rate from stage j ($mol\,s^{-1}$)
$x'_{i,j}$	mole fraction of component i on stage j, liquid phase 1
$x''_{i,j}$	mole fraction of component i on stage j, liquid phase 2
$y_{i,j}$	mole fraction of component i on stage j, vapor phase
$z_{i,j}^{\alpha\beta}$	mole fraction i on stage j, phase α at $\alpha\beta$ phase interface

Greek letters

β	phase split fraction
$\delta_{i,k}$	kronecker delta
ε	convergence tolerance
ε_v	vapor holdup
γ_i	activity coefficient of component i
$\Gamma_{i,k}$	thermodynamic factor for binary pair i and k
η	dimensionless film coordinate
φ	volumetric flow rate ($m^3\,s$)
$\kappa_{i,k}$	binary pair mass transfer coefficient components i and k ($m\,s^{-1}$)
μ	chemical potential ($J\,mol^{-1}$)
ρ	density ($kg\,m^{-3}$)
σ	surface tension ($N\,m^{-1}$)
τ_v	vapor residence time (s)

Subscripts

i	component number
j	stage number
k	Alternative component number
t	total, summation over all components

Superscripts

F	feed quantity or property
L'_j	liquid phase 1 quantity or property
L''_j	liquid phase 2 quantity or property
LL	indicating transfer films between two liquid phases
V	vapor phase quantity or property
VL'_j	indicating transfer films between vapor and liquid phase 1
VL''_j	indicating transfer films between vapor and liquid phase 2

Hutchison, Motard, and Winter (1979). The philosophy and techniques of process modeling and simulation put forth in their monograph have pervaded all of modern process engineering to the point that this material has become part of the education of all chemical engineers (see, for example, Biegler, Grossmann, & Westerberg, 1997; Seader & Henley, 1998).

2. Review

Several important processes involve the distillation of mixtures that may form two distinct liquid phases (Doherty & Malone, 2001). In some cases, this cannot be avoided, due to the nonideal thermodynamic nature of the mixture. In other cases, phase separation is induced on purpose. There are many examples of extractive or azeotropic distillation processes, in which binary azeotropes are 'broken' by the introduction of a third component that creates a liquid–liquid

region. Much of the world's dehydrated alcohol is produced by means of heterogeneous azeotropic distillation, along with many other industrially important chemicals.

The simulation of three-phase distillation processes has long been carried out using the equilibrium stage model. The model involves material balance equations, energy balance equations, equilibrium relations, and mole fraction summation equations. Obtaining the numerical solution of these equations that can be significantly more difficult than solving the equilibrium model equations for a two-phase system. There are a number of reasons for this.

- The very high nonlinearity of the thermodynamic quantities (primarily the *K*-values) means that the numerical computations are unusually sensitive to estimates of the temperatures and compositions and convergence often is very difficult to obtain. Indeed, the availability of appropriately accurate thermodynamic models often is an important consideration.
- Although the process might be called "three-phase" distillation, there will almost certainly be a number of stages with only one liquid phase present. Thus, part of the computational problem involves finding the appropriate number of phases on each stage. Put another way, the number of equations and variables necessary to determine the operating condition of a column is not known until the problem has been (nearly) solved.
- The equilibrium stage model equations always admit a "trivial" two-phase solution; that is, one vapor and one liquid phase.

Many different algorithms for solving this set of equations have been proposed. All methods are, in one sense or another, extensions of methods that have been found useful for solving two-phase distillation problems (see, for example, Biegler et al., 1997; Seader & Henley, 1998). For example, equation oriented methods (Baden & Michelsen, 1988; Cairns & Furzer, 1990a,b,c; Ferraris & Morbidelli, 1981, 1982), a multistage flash algorithm (Ferraris & Morbidelli, 1981), "bubble-point" type methods (Block & Hegner, 1976; Ferraris & Morbidelli, 1981), "inside-out" methods in which the property evaluations are put in an outer iteration loop rather than in an inner loop as in the "bubble point" type methods (Prokopakis, Seider, & Ross, 1981; Ross & Seider, 1981; Schuil & Bool, 1985) and homotopy-continuation methods (Kovach & Seider, 1987; Woodman, 1989). Swartz and Stewart (1987) used orthogonal collocation techniques to model three-phase distillation processes. The advantages of this approach include a model that can be considerably reduced in size compared to the other approaches mentioned above, and that the structure of the model does not change as the location of multiple liquid phases changes during the solution procedure. As an aside we note here that it would be an interesting challenge to adapt the Swartz–Stewart approach to the nonequilibrium model developed in this paper.

Since the number of liquid phases present on each tray in the separation unit is not generally known, the number of equations necessary for modeling the unit cannot be determined until the actual operating conditions of the column have been determined. In some algorithms it is necessary to specify in advance which stages have two phases and which stages have three phases. This is an unsatisfactory feature of such methods that makes convergence a somewhat uncertain adventure.

The equilibrium stage model, so widely used in distillation simulation and design, does not, of course, represent reality in that few stages actually operate at equilibrium. The usual way out of this difficulty is either to use overall efficiencies or to combine an equation for "stage efficiency" with the equilibrium relations. Stage efficiencies have a more fundamental basis than overall efficiencies and, for two-phase systems, can be estimated from appropriate correlations (Lockett, 1986).

Ross and Seider (1981) attempted to overcome the problem of departures from equilibrium on three-phase trays through the introduction of Murphree-type stage efficiencies, for both sets of vapor liquid equilibrium equations on a stage. For lack of any good estimation methods or experimentally determined values, Ross and Seider (1981) provide arbitrary values for these stage efficiencies and assume that all efficiencies are equal, i.e. the two liquid phases are in equilibrium with each other. In any event, reliable prediction methods for efficiencies in three-phase systems are nonexistent. Indeed, Cairns and Furzer (1990a) explicitly warn against incorporating Murphree efficiencies into the equilibrium stage model for three-phase systems. In part, this is because the numerical value of the Murphree efficiency is highly variable, but also because it is strongly dependent on the choice of thermodynamic model (this also is true for two-phase systems, of course).

Lao and Taylor (1994) reviewed the available literature on three-phase distillation efficiencies, quoting several sources of contradictory behavior for these systems. Some studies found that the overall efficiency was not influenced by the number of liquid phases present (Grohse, McCartney, Hauer, Gerster, & Colburn, 1949; Schoenborn, Koffolt, & Withrow, 1941). However, in the discussion that accompanies the paper by Schoenborn et al. (1941) all warn against generalizing this finding. The introduction of a second liquid phase can have a strong (positive or negative) influence on mass transfer behavior. Efficiencies between 25 and 50% are not uncommon (see also Section 6). Lao and Taylor (1994) state that since low and variable stage efficiencies are to be expected, 'a model based on the assumption of equilibrium on every stage cannot hope to be able to predict column performance'. In addition, choosing the best location for decanters may only be determined if the actual compositions and the presence of two liquid phases are known. Hence it is important to be able to correctly predict the location of the stages where a second liquid phase can form. The low stage efficiencies that can occur in such columns suggest

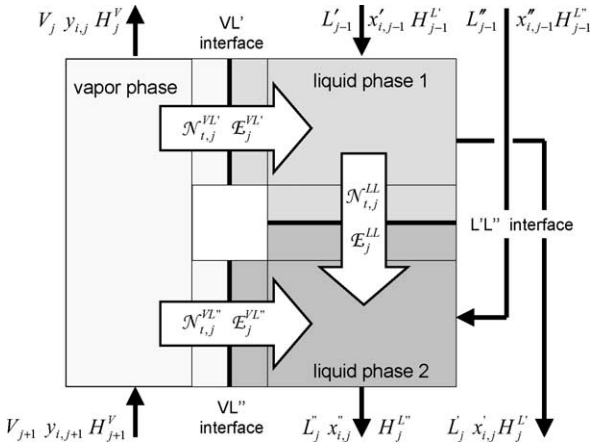

Fig. 1. Schematic representation of a three-phase stage.

that this cannot be done reliably with an equilibrium stage model.

To the best of our knowledge Lao and Taylor (1994) were the first to develop mass transfer rate-based models of three-phase distillation. However, theirs was a model for only a single tray and no attempt was made to model an entire distillation column (solving the equations for a single tray was sufficiently difficult at that time). It is the purpose of this paper to describe our nonequilibrium model of an entire three-phase distillation column and the method of solving the model equations. We address each of the topics identified in the introduction. The model framework described here and the associated computer code was used by Springer, Baur, and Krishna (2003) who found favorable agreement between with a nonequilibrium model of three-phase distillation and their own extensive set of experiments with the water (1)–cyclohexane (2)–ethanol (3) system.

3. A nonequilibrium model of three-phase distillation

The unit cell for the nonequilibrium stage model for three-phase distillation is shown in Fig. 1. This unit cell is assumed to describe a 'real' tray in a tray column or a 'real' section of packing in a packed distillation column. Present on this stage are one vapor phase and two liquid phases that may all be in contact with each other. In this figure $V_j$represents the vapor flow rate from stage j, and $L'_j$and L''_j represent the flow rates of liquid phases 1 and 2, respectively. The mole fraction of component i in the vapor stream leaving stage j is given by y_{ij}, and the mole fractions of component i in the two liquid phases present on stage j is given by x'_{ij} and x''_{ij}. The mass transfer rates are denoted by N, where the superscript $\alpha\beta$ refers to mass transfer between phase α and phase β. The energy transfer rates between the phases are denoted by E, for which a similar superscripting system is maintained. In the development of the equations, the subscript j will be reserved for stage numbering, and the subscripts i and k will be used for subscripting components. The model is developed assuming the stages are numbered from the top down, the condenser (if any) or top stage being stage 1.

3.1. Conservation equations

The overall mole (mass) balances for the vapor phase and the two liquid phases are given by:

$$V_j - V_{j+1} - F_j^{\mathrm{V}} + \mathsf{N}_{t,j}^{\mathrm{VL}'} + \mathsf{N}_{t,j}^{\mathrm{VL}''} = 0 \tag{1}$$

$$L'_j - L'_{j-1} - F_j^{\mathrm{L}'} - \mathsf{N}_{t,j}^{\mathrm{VL}'} + \mathsf{N}_{t,j}^{\mathrm{LL}} = 0 \tag{2}$$

$$L''_j - L''_{j-1} - F_j^{\mathrm{L}''} - \mathsf{N}_{t,j}^{\mathrm{VL}''} - \mathsf{N}_{t,j}^{\mathrm{LL}} = 0 \tag{3}$$

In the above equations, F represents a feed stream added to stage j. $\mathsf{N}_{t,j}^{\mathrm{VL}'}$, $\mathsf{N}_{t,j}^{\mathrm{VL}''}$, and $\mathsf{N}_{t,j}^{\mathrm{LL}}$ are the overall interphase mass transfer rates (mol/s or equivalent) between the three phases on stage j. We have omitted the primes on the LL superscripts since there is only one liquid–liquid interface.

Here, c represents the number of components. The component balances for each component in the vapor and both liquid phases are given by:

$$V_j y_{i,j} - V_{j+1} y_{i,j+1} - f_{i,j}^{\mathrm{V}} + \mathsf{N}_{i,j}^{\mathrm{VL}'} + \mathsf{N}_{i,j}^{\mathrm{VL}''} = 0 \tag{4}$$

$$L'_j x'_{i,j} - L'_{j-1} x'_{i,j-1} - f_{i,j}^{\mathrm{L}'} - \mathsf{N}_{i,j}^{\mathrm{VL}'} + \mathsf{N}_{i,j}^{\mathrm{LL}} = 0 \tag{5}$$

$$L''_j x''_{i,j} - L''_{j-1} x''_{i,j-1} - f_{i,j}^{\mathrm{L}''} - \mathsf{N}_{i,j}^{\mathrm{VL}''} + \mathsf{N}_{i,j}^{\mathrm{LL}} = 0 \tag{6}$$

In these equations, $f_{i,j}$ represents the individual component feed of component i to the phase denoted by the superscript on stage j. The energy balance equations for all three phases are given by:

$$V_j H_j^{\mathrm{V}} - V_{j+1} H_{j+1}^{\mathrm{V}} - F_j^{\mathrm{V}} H_j^{\mathrm{FV}} + \mathsf{E}_j^{\mathrm{VL}'} + \mathsf{E}_j^{\mathrm{VL}''} = 0 \tag{7}$$

$$L'_j H_j^{\mathrm{L}'} - L'_{j-1} H_{j-1}^{\mathrm{L}'} - F_j^{\mathrm{L}'} H_j^{\mathrm{FL}'} - \mathsf{E}_j^{\mathrm{VL}'} + \mathsf{E}_j^{\mathrm{LL}} = 0 \tag{8}$$

$$L''_j H_j^{\mathrm{L}''} - L''_{j-1} H_{j-1}^{\mathrm{L}''} - F_j^{\mathrm{L}''} H_j^{\mathrm{FL}''} - \mathsf{E}_j^{\mathrm{VL}''} - \mathsf{E}_j^{\mathrm{LL}} = 0 \tag{9}$$

where E represents the rate of energy transfer between phases.

3.2. Transport relations

The mass and energy transfer rates in the above conservation equations are evaluated using the Maxwell–Stefan equations here written in generic form as:

$$\frac{z_i^\alpha}{RT^\alpha}\frac{\partial \mu_i^{\alpha\beta}}{\partial \eta} = \sum_{k=1}^{c} \frac{z_i^\alpha \mathsf{N}_k^{\alpha\beta} - z_k^\alpha \mathsf{N}_i^{\alpha\beta}}{c_t^\alpha \kappa_{i,k}^{\alpha\beta} a^{\alpha\beta}} \tag{10}$$

In the above equations, α and β are phase labels chosen from V, L', L'', z_i^α is the mole fraction of species i in phase α, $\mu_i^{\alpha\beta}$ is the chemical potential of species i in the $\alpha - \beta$ film, R is the gas constant, T is the temperature, and η is a dimensionless film coordinate ($0 \le \eta \le 1$). c_t^α is the molar phase density. $\kappa_{i,k}^{\alpha\beta}$ and $a^{\alpha\beta}$ are the phase mass transfer coefficients and interfacial areas for the transport films between

phases α and β. The mole fractions in the right-hand side of the equations are the linear average of the mole fractions at the interface and in the bulk. Note that we have omitted the stage index letter j for clarity.

In the most general application of the model we need no less than six different sets of these equations; two for each possible phase boundary. Only $c-1$ of each set of these equations are independent. The mole fractions of the cth component is obtained from the summation equation (one of these equations is needed for each phase):

$$\sum_{i=1}^{c} z_{i,j}^{\alpha} - 1 = 0 \tag{11}$$

In their paper, Krishnamurthy and Taylor (1985), and later Kooijman (1995) rewrite the generalized Maxwell–Stefan (GMS) equations into an expression for a mass transfer coefficient multiplied by a driving force to obtain an expression for the mass transfer rate directly. Higler, Krishna, and Taylor (1999) used a finite difference approximation to the chemical potential gradient. Since normally, mole fraction profiles within the film and chemical potential gradients will not be very steep, the latter approach is adequate. In this model we take an even simpler approach, using just one discretisation step in the film. This means that the chemical potential gradients in Eq. (10) can be approximated by:

$$\frac{z_i^{\alpha}}{RT}\frac{\partial \mu_i^{\alpha}}{\partial \eta} = \sum_{k=1}^{c-1} \Gamma_{i,k}(z_i^{\alpha\beta} - z_i^{\alpha}) \tag{12}$$

where

$$\Gamma_{i,k} = \delta_{i,k} + z_i^{\alpha}\left(\frac{\partial \ln \gamma_i^{\alpha}}{\partial z_i^{\alpha}}\right)_{T,P,z_{i,k,k\neq j=1\ldots c-1}^{\alpha}} \tag{13}$$

For the vapor phase we may estimate the thermodynamic factor from a similar expression on which the species fugacity coefficient appears in place of the activity coefficient (Taylor & Krishna, 1993, p. 24). If, further, we assume that the vapor phase is ideal then $\Gamma_{ik} = \delta_{ik}$. The mole fractions on the right-hand side of Eq. (10) are approximated at the arithmetic average $0.5(z_i^{\alpha} + z_i^{\alpha\beta})$.

By themselves, the Maxwell–Stefan equations are 'floating' equations. They relate the driving force for mass transfer of a component to the frictional drag between different species in terms of relative velocities and drag coefficients. Eq. (14) is, therefore, required to 'tie down' these relative velocities in each of the coupled transfer films. These equations are commonly referred to as the bootstrap condition (Krishna & Wesselingh, 1997; Taylor & Krishna, 1993; Wesselingh & Krishna, 2000).

$$\begin{aligned}\mathsf{E}_j^{\alpha\beta} &= -h_j^{\alpha\beta} a_j^{\alpha\beta}(T_j^{\alpha} - T_j^{\alpha\beta}) + \sum_{i=1}^{c} \mathsf{N}_{i,j}^{\alpha\beta} \bar{H}_{i,j}^{\alpha\beta} \\ &= -h_j^{\beta\alpha} a_j^{\alpha\beta}(T_j^{\alpha\beta} - T_j^{\beta}) + \sum_{i=1}^{c} \mathsf{N}_{i,j}^{\alpha\beta} \bar{H}_{i,j}^{\beta\alpha}\end{aligned} \tag{14}$$

where $T^{\alpha\beta}$ represents the temperature of the $\alpha-\beta$ interface, h is a heat transfer coefficient, and $\bar{H}$ the partial molar enthalpy. The difference $\bar{H}_{i,j}^{\alpha\beta} - \bar{H}_{i,j}^{\beta\alpha}$ represents the molar heat of vaporization. This factor is important only for vapor–liquid mass transfer. For liquid–liquid mass transfer, the partial molar latent heats will be nearly equal and the bootstrap equation essentially requires the conductive heat fluxes to be the same (although the full interfacial energy balance (14) is used in the calculations).

3.3. Interface equations

Thermodynamic equilibrium is assumed at the interfaces between two distinct phases.

$$\begin{aligned} &z_{i,j}^{\alpha\beta} = K_{i,j}^{\alpha\beta} z_{i,j}^{\beta\alpha}, \qquad \alpha \in \{V, L', L''\}, \\ &\alpha \neq \beta \in \{V, L', L''\}\end{aligned} \tag{15}$$

where $z_{i,j}^{\alpha\beta}$ is the mole fraction of species i in the α phase at the $\alpha\beta$ phase boundary. There are three possible interfaces and, therefore, three sets of these equilibrium relations are required.

Note here, that, since it is not assumed that three phases are at equilibrium at any particular point in the three-phase mixture, the above three equations are completely independent. This is in contrast to the equilibrium stage model, in which only two independent sets of equilibrium relations exist.

In addition, it is necessary that the mole fractions at all interfaces in all phases should sum up to unity:

$$\begin{aligned} &\sum_{i=1}^{c} z_{i,j}^{\alpha\beta} - 1 = 0, \qquad \alpha \in \{V, L', L''\}, \\ &\alpha \neq \beta \in \{V, L', L''\}\end{aligned} \tag{16}$$

3.4. Hydraulic equation

The pressure may be evaluated from the pressure on the stage above and the pressure drop over the stage.

$$P_j = P_{j-1} + \Delta P_{j-1} \tag{17}$$

3.5. Reboiler and condenser

The reboiler and condenser will be modeled as equilibrium stages. For each three-phase equilibrium stage, the total mass balance is given by:

$$V_j - V_{j+1} + L_j' - L_{j-1}' + L_j'' - L_{j-1}'' - F_j = 0 \tag{18}$$

The individual component balances are given by:

$$\begin{aligned} &V_j y_{i,j} - V_{j+1} y_{i,j+1} + L_j' x_{i,j}' - L_{j-1}' x_{i,j-1}' + L_j'' x_{i,j}'' \\ &\quad - L_{j-1}'' x_{i,j-1}'' - f_{i,j} = 0\end{aligned} \tag{19}$$

The overall energy balance of an equilibrium stage is given by:

$$V_j H^{\mathrm{V}}_{i,j} - V_{j+1} H^{\mathrm{V}}_{i,j+1} + L'_j H^{\mathrm{L}'}_{i,j} - L'_{j-1} H^{\mathrm{L}'}_{i,j-1} + L''_j H^{\mathrm{L}''}_{i,j} - L''_{j-1} H^{\mathrm{L}''}_{i,j-1} - F_j H^{\mathrm{F}}_j + Q_j = 0 \quad (20)$$

In which Q_j is a heat duty that may be specified to the stage. In addition, phase equilibrium is assumed between the bulk phases of the vapor and the two liquid phases:

$$y_{i,j} = K'_{i,j} x'_{i,j}, \quad y_{i,j} = K''_{i,j} x''_{i,j}, \quad x'_{i,j} = K^{\mathrm{L}}_{i,j} x''_{i,j} \quad (21)$$

Only two of the above three equilibrium correlations are independent: the first and second parts of Eq. (21) may be divided to give the third part, with

$$K^{\mathrm{L}}_{i,j} = \frac{K''_{i,j}}{K'_{i,j}} \quad (22)$$

In addition, it is necessary that the mole fractions of the components in each individual phase sum up to 1:

$$\sum_{i=1}^{c} y_{i,j} = 1, \qquad \sum_{i=1}^{c} x'_{i,j} = 1, \qquad \sum_{i=1}^{c} x''_{i,j} = 1 \quad (23)$$

The pressure in the reboiler may be calculated from the pressure on the bottom stage:

$$P_j = P_{j-1} + \Delta P \quad (24)$$

The pressure of the condenser has to be specified:

$$P_1 = P_{\mathrm{spec}} \quad (25)$$

3.6. Transition stages

It is likely that a column will have some trays on which only one liquid phase is present. For example, it is possible for a tray to receive liquid from both phases on the tray above, but only one liquid phase leaves or for two liquid phases to leave a stage while receiving a single liquid phase from the stage above. These situations are depicted in Fig. 2. In case a three-phase stage dumps two liquids onto a two-phase stage, the mass balance for the three-phase stage does not change, but the mass balance for the two-phase stage becomes:

$$L'_j - L'_{j-1} - L''_{j-1} - F^{\mathrm{L}'}_j - \mathsf{N}^{\mathrm{VL}}_{i,j} = 0 \quad (26)$$

The term for mass transfer to the second liquid phase has disappeared. The component mass balance becomes:

$$L'_j x'_{i,j} - L'_{j-1} x'_{i,j-1} - L''_{j-1} x''_{i,j-1} - f^{\mathrm{L}'}_{i,j} - \mathsf{N}^{\mathrm{VL}}_{i,j} = 0 \quad (27)$$

The energy balance for this situation is:

$$L'_j H^{\mathrm{L}'}_j - L'_{j-1} H^{\mathrm{L}'}_{j-1} - L''_{j-1} H^{\mathrm{L}''}_{j-1} - F^{\mathrm{L}'}_j H^{\mathrm{FL}'}_j - \mathsf{E}^{\mathrm{VL}'}_j = 0 \quad (28)$$

The equations do not need to be modified for the case in which a two-phase stage supplies liquid to a three-phase stage. It is, however, necessary to 'add' the liquid phase to the 'correct' liquid phase. We assume that the liquid from the stage above is added to the liquid phase on the stage below to which it is closest in proximity in composition space. For this, the following composition distance function is evaluated for both liquid phases present on the three-phase stage.

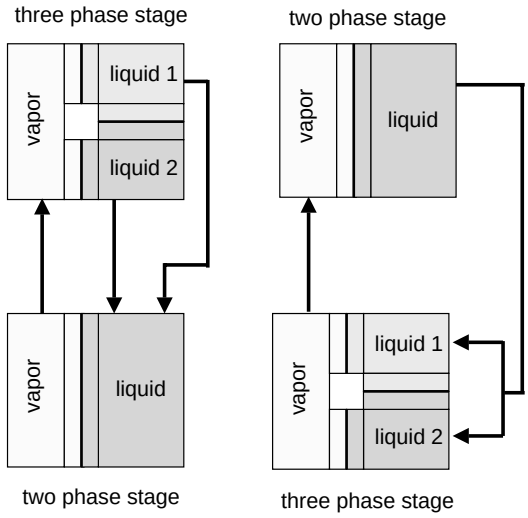

Fig. 2. Three-phase to two-phase, and two-phase to three-phase stages.

$$\Delta x^{\alpha} = \sqrt{\sum_{i=1}^{c} (x_{j-1} - x^{\alpha}_j)^2} \quad (29)$$

The liquid from the stage above is added to the liquid with the smallest value of the distance function. The result of adding the liquid to the 'wrong' phase is unreasonably high predictions of mass transfer rates because the driving forces (composition differences) are abnormally large.

3.7. Mass transfer coefficients

One of the important issues encountered in nonequilibrium modeling of three-phase distillation is the absence of methods for estimation of mass and heat transfer coefficients and interfacial areas. Closely related to the issue of mass transfer is that of the nature of the contact between the phases.

Lao and Taylor (1994) proposed four simple flow models (of varying degrees of realism). Here we focus on two contacting models, as shown in Fig. 3. In model 1, it is assumed that the vapor only sees one liquid phase. The other liquid phase is completely dispersed within the continuous liquid. This means that one set of mass transfer equations for vapor liquid contacting may be removed from the above set of equations.

In contact model 2 (the stratified flow model) the vapor sees both liquid phases in turn. There would be negligible mass transfer between the two liquids. Photographs published by Davies, Ali and Porter (1987) suggest that this flow regime might sometimes occur in practice, but the dis-

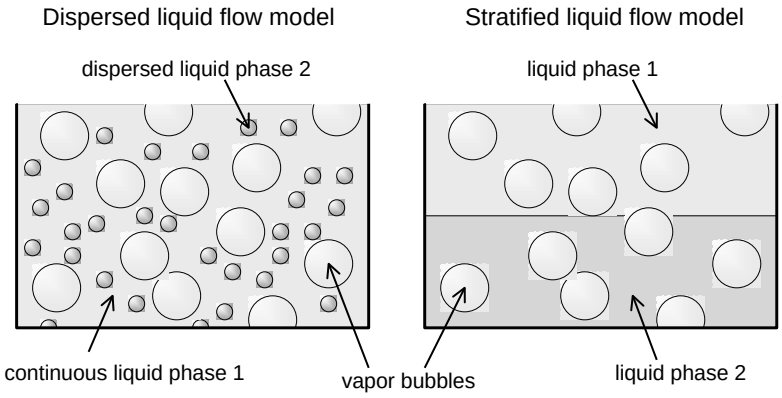

Fig. 3. Possible contacting models in three-phase distillation.

persed liquid phase has been observed more frequently in experimental studies (although it must be admitted that the number of such studies remains quite small in number).

Springer et al. (2003), who used the framework described here and the computer code developed for this work to simulate their own experiments involving the mixture water–ethanol–cyclohexane, employed the dispersed liquid model and assumed that the two liquid phases were in equilibrium with each other. This means that the liquid–liquid mass transfer rate equations can be eliminated (or replaced by equations that set the bulk liquid composition equal to the liquid–liquid interface composition).

In the absence of generally applicable empirical correlations for the mass transfer coefficients Springer et al. (2003) assumed that the vapor phase rises through the liquid phase as a swarm of uniform, spherical bubbles with a diameter d_b. The liquid (froth) phase is assumed to have a uniform thickness of h_f. The vapor liquid interfacial area per unit volume of vapor is given by:

$$a_v = \frac{6}{d_b} \tag{30}$$

The residence time of the vapor in the liquid (froth) film is:

$$\tau_v = \frac{h_f}{v_b} \tag{31}$$

In which v_b is the bubble rise velocity, and is estimated from (Mendelson, 1967)

$$v_b = \sqrt{\frac{2\sigma}{\rho_L d_b} + \frac{g d_b}{2}} \tag{32}$$

The vapor phase mass transfer coefficients may be evaluated *for each binary pair* of species from the following equation for unsteady-state diffusion within a spherical bubble:

$$Sh_{i,k} = \frac{\kappa^V_{i,k} d_b}{\mathcal{D}^V_{i,k}} = \frac{2\pi^2}{3}\left(\frac{\sum_{m=1}^{\infty}\exp\{-m^2\pi^2 Fo_{i,k}\}}{\sum_{m=1}^{\infty}(1/m^2)\exp\{-m^2\pi^2 Fo_{i,k}\}}\right) \tag{33}$$

with

$$Fo_{i,k} = \frac{4\mathcal{D}^V_{i,k}\tau_v}{d_b^2} \tag{34}$$

For Fourier numbers larger than about 0.06, the Sherwood number reduces to the asymptotic value of $2\pi^2/3$ and the steady-state binary pair mass transfer coefficients for the vapor phase are given by:

$$\kappa^V_{i,k} = \frac{2\pi^2}{3}\frac{\mathcal{D}^V_{i,k}}{d_b} \tag{35}$$

The liquid phase mass transfer coefficients are obtained from a penetration model, leading to:

$$\kappa^L_{i,k} = 2\sqrt{\frac{\mathcal{D}^L_{i,k}}{\pi t_c}} \tag{36}$$

in which the contact time between the liquid with the gas t_c is given by:

$$t_c = \frac{d_b}{v_b} \tag{37}$$

In the above set of equations, there are two parameters that have to be specified: the froth height and the bubble diameter. When modeling an actual process for which data is available these parameters can be chosen to best fit the measurements.

The total interfacial area between vapor and liquid per m^2 of bubbling area (required in the MS equations) is obtained from:

$$a_{int} = a_v \varepsilon_v h_f \tag{38}$$

where ε_v is the vapor holdup on a tray which may be obtained from $\varepsilon_f = u_v/v_b$ where u_v is the superficial gas velocity, and v_b is the bubble rise velocity.

3.8. Total reflux calculations

A modification of this procedure is needed in order to be able to simulate distillation operations at total reflux (a

condition encountered many times in experimental studies). In effect, total reflux means that a degree of freedom is lost, since the column has no feed and delivers no product. For total reflux simulations, compositions on one tray are set to those measured in the experiments. This means that the component balances for the designated stage are replaced by specification equations for the (known) mole fractions. In addition, the bottom product flow rate is set to zero. The last degree of freedom is removed by specifying the reflux flow rate.

4. Degrees of freedom analysis

To model a complete three-phase distillation column four possible types of stage may be needed.

1. A nonequilibrium three-phase stage.
2. A nonequilibrium two-phase stage.
3. An equilibrium three-phase stage.
4. An equilibrium two-phase stage.

4.1. Equations and variables

The variables for the nonequilibrium stages are summarized in Table 1. The variables summarized in the first six lines of the table are the variables for a two-phase nonequilibrium stage. The additional variables for a nonequilibrium three-phase stage appear following the 6th line of the table. The number of variables for a two-phase stage is $5c+6$, the number of variables for a nonequilibrium three-phase stage is $12c+10$. The variables for an equilibrium stage are summarized in Table 2. The number of variables for a two phase stage is $2c+4$ and for a three-phase stage $3c+6$.

Table 1
Variables for a nonequilibrium stage

Variable	Symbol	Number
Vapor flow rate	V_j	1
Liquid flow rate phase 1	L'_j	1
Liquid flow rate phase 2	L''_j	1
Vapor phase bulk composition	$y_{i,j}$	c
Liquid phase 1 bulk composition	$x'_{i,j}$	c
Liquid phase 2 bulk composition	$x''_{i,j}$	c
Vapor interface composition (vapor–liquid 1)	$y_{i,j}^{\mathrm{VL}'}$	c
Liquid interface composition (vapor–liquid 1)	$x_{i,j}^{\mathrm{L}'\mathrm{V}}$	c
Vapor interface composition (vapor–liquid 2)	$y_{i,j}^{\mathrm{VL}''}$	c
Liquid interface composition (vapor–liquid 2)	$x_{i,j}^{\mathrm{L}''\mathrm{V}}$	c
Liquid 1 interface composition (liquid–liquid)	$x_{i,j}^{\mathrm{L}'\mathrm{L}''}$	c
Liquid 2 interface composition (liquid–liquid)	$x_{i,j}^{\mathrm{L}''\mathrm{L}'}$	c
Vapor phase bulk temperature	T_j^{V}	1
Liquid phase 1 bulk temperature	$T_j^{\mathrm{L}'}$	1
Liquid phase 2 bulk temperature	$T_j^{\mathrm{L}''}$	1
Interface temperature vapor–liquid 1	$T_j^{\mathrm{VL}'}$	1
Interface temperature vapor–liquid 2	$T_j^{\mathrm{VL}''}$	1
Interface temperature liquid–liquid	T_j^{LL}	1
Stage pressure	P_j	1
Mass transfer rates vapor–liquid 1	$\mathsf{N}_{i,j}^{\mathrm{VL}'}$	c
Mass transfer rates vapor–liquid 2	$\mathsf{N}_{i,j}^{\mathrm{VL}''}$	c
Mass transfer rates liquid 1–liquid 2	$\mathsf{N}_{i,j}^{\mathrm{L}'\mathrm{L}''}$	c

Table 2
Variables for an equilibrium stage

Variable	Symbol	Number
Vapor flow rate	V_j	1
Liquid flow rate phase 1	L'_j	1
Liquid flow rate phase 2	L''_j	1
Vapor phase composition	$y_{i,j}$	c
Liquid phase 1 composition	$x'_{i,j}$	c
Liquid phase 2 composition	$x''_{i,j}$	c
Stage temperature	T_j	1
Stage pressure	P_j	1
Stage heat duty	Q_j	1

The equations to be solved for each nonequilibrium stage are summarized in Table 3. For each stage there is a total of $5c+6$ equations for each two-phase stage and a total of $12c+10$ equations for each three-phase stage. The equations for the equilibrium stages are summarized in Table 4.

Table 3
Equations for a nonequilibrium stage

Equation	Reference	Number
Vapor phase mass balance	(1)	1
Liquid phase 1 mass balance	(2)	1
Liquid phase 2 mass balance	(3)	1
Vapor phase component balance	(4)	$c-1$
Liquid phase 1 component balance	(5)	$c-1$
Liquid phase 2 component balance	(6)	$c-1$
Vapor bulk summation equation	(11)	1
Liquid 1 bulk summation equation	(11)	1
Liquid 2 bulk summation equation	(11)	1
Vapor energy balance	(11)	1
Liquid 1 energy balance	(11)	1
Liquid 2 energy balance	(11)	1
Equilibrium vapor/liquid 1	(15)	c
Equilibrium vapor/liquid 2	(15)	c
Equilibrium liquid/liquid	(15)	c
MS–vapor film at liquid phase 1	(10)	$c-1$
MS–vapor film at liquid phase 2	(10)	$c-1$
MS–liquid phase 1 film at vapor phase	(10)	$c-1$
MS–liquid phase 1 film at liquid phase	(10)	$c-1$
MS–liquid phase 2 film at vapor phase	(10)	$c-1$
MS–liquid phase 2 film at liquid phase	(10)	$c-1$
Bootstrap vapor–liquid 1	(14)	1
Bootstrap vapor–liquid 2	(14)	1
Bootstrap liquid 1–liquid 1	(14)	1
Summation equation vapor phase, at liquid phase 1	(16)	1
Summation equation vapor phase, at liquid phase 2	(16)	1
Summation equation liquid phase 1 at vapor phase	(16)	1
Summation equation liquid phase 1 at liquid phase	(16)	1
Summation equation liquid phase 2 at vapor phase	(16)	1
Summation equation liquid phase 2 at liquid phase	(16)	1
Hydraulic equation	(17)	1

Table 4
Equations for an equilibrium stage

Equation	Reference	Number
Total mass balance	(18)	1
Component mass balances	(19)	$c - 1$
Total energy balance	(20)	1
Summation equation vapor phase	(23)	1
Equilibrium equations vapor–liquid 1	(21)	c
Summation equation liquid phase 1	(23)	1
Pressure equation	(24)	1
Equilibrium equations vapor–liquid 2	(21)	c
Summation equation liquid phase 2	(23)	1

4.2. Degrees of freedom

The total number of equations and variables for three-phase nonequilibrium stages is $12c + 10$ and for two-phase stages is $5c + 6$. There are, therefore, no degrees of freedom on these stages. The total number of equations for an equilibrium stage with three phases is $3c + 5$ and with two phases $2c + 4$. The total number of variables is $3c + 6$ for three-phase stages and $2c + 5$ for two-phase stages, resulting in one degree of freedom per equilibrium stage. For the reboiler and condenser, normally the energy balance is replaced by a specification equation on, for example, the reflux, the boilup ratio, or the product purity.

4.3. Specifications

4.3.1. Configuration

The configuration of the column needs to be fixed. This requires the specification of the number of stages, number of feeds and their locations, number of (decanted) side streams and their locations, and possible external heat duties.

4.3.2. Pressure model and condenser pressure

The condenser pressure needs to be specified. In addition, it is common practice to give an independent specification for the top stage, since the top stage pressure may differ substantially from the condenser pressure, depending on the design used. Furthermore, a pressure drop model needs to be specified for each nonequilibrium stage. Possible options are as follows.

- No pressure drop—all stages in the column are at the same pressure.
- Fixed pressure drop—the pressure drop is assumed to be equal for all stages, and the stage pressure may be calculated from the top pressure and the pressure drop over all stages above the stage under consideration.
- Fixed top and bottom pressure. The pressure profile is interpolated between the specified top and bottom pressures.
- Estimated pressure drop. The pressure drop is estimated from a semi-empirical correlation.

4.3.3. Feeds

Specification of flow rate, composition and thermodynamic state of each feed is required. The latter can be determined if any of the two following parameters are specified: pressure, temperature and vapor fraction.

4.3.4. Decanted side streams

For each decanted side stream, one needs to specify which phase is decanted. In practice this is handled by specifying a component that consists mainly in the decanted stream (e.g. water for a watery stream, or an organic component for an organic phase).

4.3.5. Thermodynamic models

Specification of a thermodynamic model is required for the calculation of, among other things, chemical potential gradients, vapor–liquid and liquid–liquid equilibrium. With respect to the vapor–liquid and liquid–liquid equilibrium, it should be noted that all three sets of Eq. (15) are independent. This means that the three-phase nonequilibrium model does not assume that the three phases present on a stage exist at equilibrium. It is assumed that, at an interface, only two phases come into contact at any particular place and time. Equilibrium is only assumed at the interface. As a consequence, it is possible to use different thermodynamic models for each phase equilibrium calculation (Lao & Taylor, 1994). A benefit of this is that LL equilibrium may be evaluated using coefficient model parameters that were fitted to LLE data, and VL equilibrium may be evaluated using parameters fitted to VLE data. This circumvents the need for accurate VLLE data and models that are able to accurately describe these VLLE characteristics. This is contrary to an equilibrium three-phase model, the quality of which strongly hinges on the ability of the thermodynamic models to accurately describe VLLE. However, for equilibrium stages it is necessary to use the same models and parameters in order to preserve thermodynamic consistency.

4.3.6. Mass transfer model

The following parameters have to be specified for the mass transfer model.

- The bubble diameter.
- The froth height.
- The contacting model, and related to that, which liquid phase gets to see the vapor phase or how much of the liquid phase gets to ‘see’ the vapor phase.
- Liquid droplet diameter (only if the liquid phases are not assumed in equilibrium with each other.

4.3.7. Other physical properties

A nonequilibrium model also requires information about properties such as surface tension, density and heat capacity. These properties are needed for the estimation of mass transfer coefficients (and possibly for pressure-drop and interfacial area calculations).

The overall liquid density may be evaluated as the weighed average of the liquid densities:

$$\rho_{\mathrm{L}}^{\mathrm{av}} = \frac{\phi^{\mathrm{L}'}\rho_{\mathrm{L}'} + \phi^{\mathrm{L}''}\rho_{\mathrm{L}''}}{\phi^{\mathrm{L}'} + \phi^{\mathrm{L}''}} \tag{39}$$

in which $\phi^{\mathrm{L}'}$ and $\phi^{\mathrm{L}''}$ are the volumetric flow rates of liquid phase 1 and liquid phase 2, respectively. This averaging is justified if the two phases form a fine dispersion. If two distinct layers are formed on the tray it may be better to split up the VL mass transfer calculation into two steps, one from the vapor to the 'heavy' liquid phase, and secondly, from the vapor to the 'light' liquid phase. There is no difficulty with Eq. (39) near a liquid–liquid critical point; the densities of the two liquid phases will then be more nearly equal and Eq. (39) becomes a much better approximation.

For the surface tension, things are less straightforward. The mixture surface tension of both liquid phases may be estimated with established methods for VL systems as described in Poling, Prausnitz, and O'Connell (2001). One could argue that as long as the vapor 'sees' only one liquid the surface tension to be used is the surface tension of that phase, and the density is the averaged liquid density.

5. Comparison with other models

A small number of other investigators have used the Lao–Taylor model as the basis of or starting point for the development of three-phase column models. These works are reviewed below now that we are better placed to be able to comment on these models.

Eckert and Vanek (2001) have described an unsteady-state nonequilibrium model largely based on a simplified version of the steady-state model of Lao and Taylor, in which they assume that one liquid phase is completely dispersed in the other phase. The dispersed liquid phase does not 'see' the vapor phase, and there are no mass or heat transfer resistances between the two liquid phases. As a consequence, the two liquid phases are always in equilibrium with each other. Eckert and Vanek implement their equations within RATEFRAC from Aspen Tech and use the *AIChE* method for estimation of mass transfer coefficients (see chapter 12 of Taylor & Krishna, 1993), and the Chilton–Colburn analogy for heat transfer coefficients. Note that they only calculate mass transfer between the vapor and the continuous liquid phase. It should be noted that their paper does not discuss the issue of transition from single liquid phase to two liquid phases at points that are not known.

A model described by Mortaheb, Kosuge, and Asano (2002) assumes equilibrium between the two liquid phases. An unusual aspect of their model is that the mass transfer rate equations are expressed in terms of mass factions rather than the mole fractions that are more commonly used; the latter are much easier to work with, especially in the strongly nonideal systems that are encountered in three-phase systems. Their model appears to have been developed more as an aide to interpreting their own experimental studies noted above than as a process design and simulation tool.

Repke and Wozny (2001, 2002) have conducted an experimental investigation of three-phase distillation in a column equipped with structured packing. They do not present many details of their model, but it appears to be based on the stage model of Lao and Taylor (1994) with appropriate changes to deal with the rather different hydrodynamic conditions in a packed column. Mass transfer coefficients in the vapor–liquid interfaces are estimated from empirical correlations developed for two phase system; those for the liquid–liquid interface from film theory (which implies that an estimate of the film thickness somehow is provided). No details on various interfacial areas are given, but this is an important parameter in nonequilibrium modeling.

6. Solving the model equations

The basic strategy we employ for solving the three-phase NEQ problem is as follows.

- Solve an equivalent two-phase equilibrium stage problem. By equivalent we mean a system having the same number of stages and similar specifications.
- Solve an equivalent three-phase equilibrium stage problem (the solution to step 1 provides an initial point of sorts from which to begin these calculations as discussed below).
- Solve the complete three-phase NEQ model (the solution to step 2 again providing a starting point of sorts).

In what follows we elaborate upon this procedure (which has proven to be quite fast and reliable even on a rather ordinary PC).

6.1. Parts I and II

For each part of the procedure outlined above we must select an appropriate strategy for solving the model equations: an equation tearing approach, or an equation oriented approach (see Biegler et al., 1997 or Seader & Henley, 1998 for background). An additional complication here is that the structure of the system of equations in steps 2 and 3 is not known in advance of the solution. This is due to the fact that we do not know the location of those stages that will have two liquid phases (and which are modeled by the three-phase NEQ model described here) and those stages with just a single liquid phase and are modeled by the conventional NEQ model (not forgetting the transition stages modeled as described above). This additional complication is not encountered during the solution of the equations that model two-phase systems (part 1). It might be argued that the lack of a defined equation structure would favor an equation tearing approach as a class of method that can adapt more easily to an evolving problem structure. However, we have long preferred equation-oriented strategies for solving NEQ

model equations (Powers et al., 1988) and, with appropriate modifications, will adopt such a strategy again here.

The first part of the algorithm is to solve a simplified version of the real problem, a two-phase equilibrium stage model. A more or less standard equation-oriented approach is used for this calculation (complete details are given by Kooijman and Taylor (2001).

A special continuation method has been developed for going from the equilibrium two-phase to the equilibrium three-phase solution. Following convergence of the equilibrium stage model, a thermodynamic phase stability calculation as outlined below is carried out for each liquid stream. In case there are any unstable liquid phases, a liquid–liquid flash is employed to calculate the compositions of the two liquid phases present on a stage. These results are subsequently used in the initialization of the three-phase equilibrium stage model. The liquid–liquid flash does not change the overall composition of the mixture, and the mass, component and energy balances will still be satisfied after the LL flash. In addition, because the LL flash calculates the compositions of the liquid phases in equilibrium with each other, the liquid–liquid equilibrium equations will be satisfied as well. The only equations that will, in the first iteration, not be satisfied, are the vapor–liquid equilibrium equations. These may, however, be forced to be satisfied by means of the introduction of a vaporization efficiency:

$$E^{V}_{i,j} = \frac{y_{i,j}}{K_{i,j}x_{i,j}} \tag{40}$$

where x and y refer the liquid and vapor mole fractions in a two phase equilibrium stage model. This vaporization efficiency is entered into the vapor–liquid equilibrium equations by means of the following equation:

$$y_{i,j} = ((1-t)E^{V}_{i,j} + t)K_{i,j}x_{i,j} \tag{41}$$

in which t is a continuation parameter. By moving systematically from $t = 0$–1, the original problem is converted into the three-phase equilibrium problem. Note that the vaporization efficiency in Eq. (41) disappears at $t = 1$. Continuation methods for solving distillation models are now widely used in process simulation (see Seader, 1985 for background).

Decanted side streams may be handled in a similar way. The problem with decanted side streams is that they can only exist when there are two liquid phases present on a tray. This means that decanted side streams can only be introduced after the two-phase equilibrium problem has been solved, and the liquid on all stages has been analyzed for stability. The introduction of a decanted side stream normally results in substantial changes in the column flow and composition profiles that may lead to failure of the numerical algorithm to provide a converged solution. A continuation method has been devised for introducing a decanted side stream in order to avoid these problems. Initially, the decanted side stream is considered to be a normal side stream, the magnitude of which may be estimated based on the total feed stream of the main constituents of the phase to be decanted. In the three-phase flash, the decanted side stream may then be gradually introduced by means of a continuation method. The combination of these two steps (the two-phase equilibrium stage model followed by a three-phase equilibrium stage model) provides a good initial guess for the three-phase nonequilibrium model.

6.2. Part III

The calculations for parts I and II can be considered to be a fairly sophisticated way of estimating most of the unknown variables for the solution of the three-phase NEQ model equations. The numerical method we prefer for solving these equations is a largely unconstrained Newton's method (we also use this method for the two-phase equilibrium stage problem in step 1, the liquid phase stability problem and liquid–liquid flash calculations, the three-phase equilibrium stage problem in part II).

In our implementation of Newton's method to solve the model equations it is necessary to allow for the number of equations (and variables) to change during the course of the solution procedure as the number of liquid phases changes between iterations. We have made no attempt to constrain such changes, allowing the method to adapt the number of model equations and the structure at will.

6.3. Stability analysis

The stability of the liquid phase as it leaves each stage must be determined each iteration during parts 2 and 3 of the procedure outlined above. Thus, as part of our simulation model the phase stability test as devised by Michelsen (1982a,b) has been implemented. This calculation, although by no means always an easy one to converge, has been well described in the literature and we refer readers to the original papers of Michelsen (1982a,b) and to Smith, Missen, and Smith (1993) for details. If the liquid phase is found to be unstable, we solve a liquid–liquid flash problem to find the composition of each liquid phase. Phase separation takes place when the phase is thermodynamically unstable; it is not a mass transfer operation. Thus, there is no inconsistency in the model created by using a phase equilibrium calculation in this context. The initial estimates for the liquid–liquid flash are obtained from the aforementioned stability calculation. The model has been used to test for the presence of "only" two liquid phases for which the Michelsen method has been found to adequate. It might be worth noting that phase stability and phase split calculations for a distillation column are easier than isolated liquid–liquid flash calculations. In a distillation column, compositions from the stages above or below that under consideration can also be used to refine the initial estimates, thereby improving the chances of success.

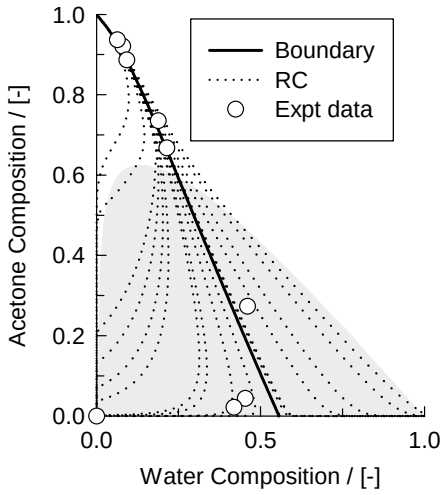

Fig. 4. Residue curve map for the water (1)–acetone (2)–toluene (3) system along with the experimental data (open circles representing the vapor compositions) for Run WAT-1 of Springer et al. (2003). The grey shaded areas represent the region in which liquid–liquid phase splitting occurs. The thick line represents the distillation boundary.

7. Some simulation results

Springer et al. (2003) have already demonstrated that the NEQ model and method of solution described above works. The results of the nonequilibrium model were compared with data obtained in an extensive experimental investigation. In general, a good match between numerical data and experiments was obtained. The NEQ model is able to predict both the crossing and the non-crossing of equilibrium distillation boundaries when such events are observed in the experiments whereas the EQ model predicts the exact opposite (in both situations). The computational procedure proved reliable and quite fast, even on a rather ordinary PC.

7.1. Water–acetone–toluene system

Consider the experimental data of Springer et al. (2003) during total reflux distillation of water–acetone–toluene in a bubble-cap tray distillation. Their published data for Run WAT-1 is plotted in the composition triangle, along with the residue curve (RC) in Fig. 4. The system shows one minimum boiling heterogeneous azeotrope between water and toluene and a straight distillation boundary connecting the azeotrope with pure acetone. The experimentally measured composition trajectory is particularly intriguing in that as we move from the condenser end (nearly pure acetone) the composition line seems to lie to the right of the distillation boundary but as the reboiler is approached the compositions move away from the water rich regions and ends up yielding nearly pure toluene in the reboiler.

We have simulated this column using both the NEQ and EQ models. For the NEQ model, we assumed that the two liquid phases are in equilibrium. The bubble diameter is taken to be 2.5 mm. This figure was not chosen arbitrarily; rather, it is derived from binary distillation experiments performed by Springer et al. (2003). The composition profiles of (a) water; (b) acetone; and (c) toluene predicted by the two models are shown in Fig. 5, along with the experimental data. For total reflux simulations we need to define a "starting" composition; in our simulations we took the vapor composition leaving stage 9 as input data. We see that the EQ model follows the trajectory dictated by the residue curve and predicts a reboiler rich in water. The NEQ model rightly anticipates the boundary crossing phenomena and predicts a toluene rich reboiler.

In order to appreciate the reason behind the sharp change in the column trajectories predicted by the EQ and NEQ models we have back calculated the Murphree component efficiencies from the NEQ simulations. The Murphree efficiency of each component can be calculated from the results

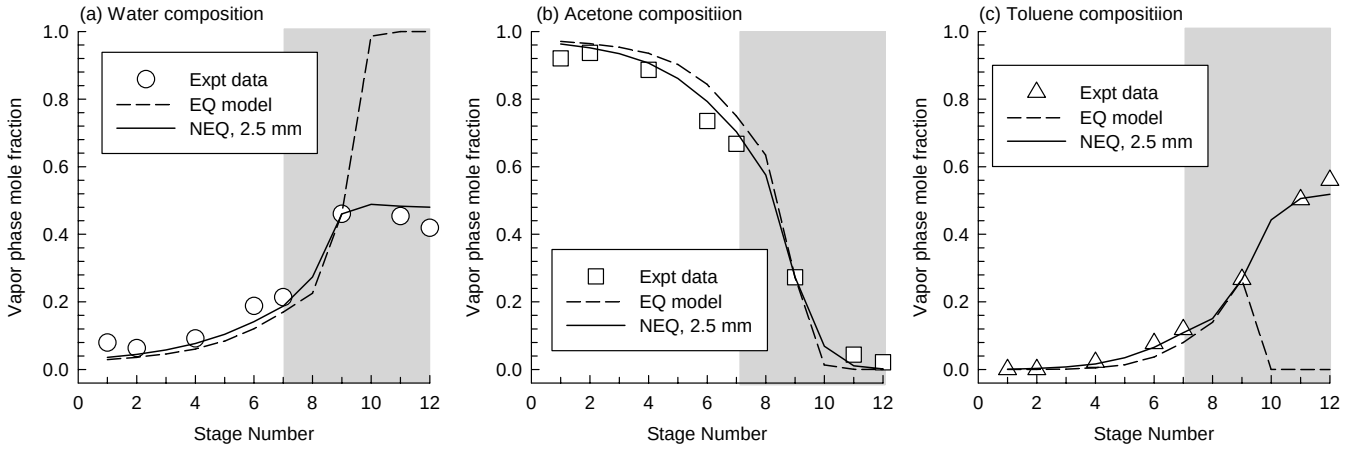

Fig. 5. Experimental vapor compositions along the distillation column for (a) water; (b) acetone; and (c) toluene. Also shown are the simulation results showing the trajectories calculated by the EQ stage model (100% efficiency) and the NEQ stage model. In the NEQ model simulations a bubble size $d_b = 2.5$ mm was chosen. The grey shaded areas represent the stages on which liquid–liquid phase splitting occurs.

of a simulation by:

$$E_i^{\mathrm{MV}} = \frac{y_{i,\mathrm{L}} - y_{i,\mathrm{E}}}{y_i^* - y_{i,\mathrm{E}}} \tag{42}$$

where the subscripts E and L refer to the composition of streams entering and leaving a stage and where y_i^* is the composition of a vapor in equilibrium with the leaving liquid phase. If the two liquids are not in equilibrium with each other then we must define two independent sets of efficiencies and interpreting the results becomes very difficult indeed. In this case we do assume that the liquid phases are in equilibrium—an assumption supported by the NEQ simulation results (Springer et al., 2003). This requires a three-phase equilibrium calculation to determine y_i^* but this is fairly straightforward.

The component efficiency profiles are shown in Fig. 6. From stages 2 to 7, the liquid phases on the trays are homogeneous, and the component efficiencies are close to one another. The situation changes dramatically as soon as the liquid–liquid region is entered. The component efficiencies show a wide variation from stage to stage. For toluene the efficiency is 550% on stage 10; this drops to −45% on stage 11. The large positive efficiency of toluene helps it to cross

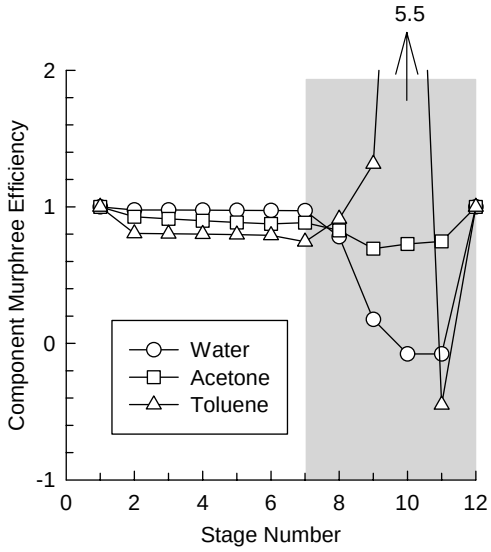

Fig. 6. Component Murphree efficiencies predicted by the NEQ stage model for distillation of water–acetone–toluene at total reflux. In the NEQ model simulations a bubble size $d_b = 2.5$ mm was chosen. The grey shaded areas represent the stages on which liquid–liquid phase splitting occurs.

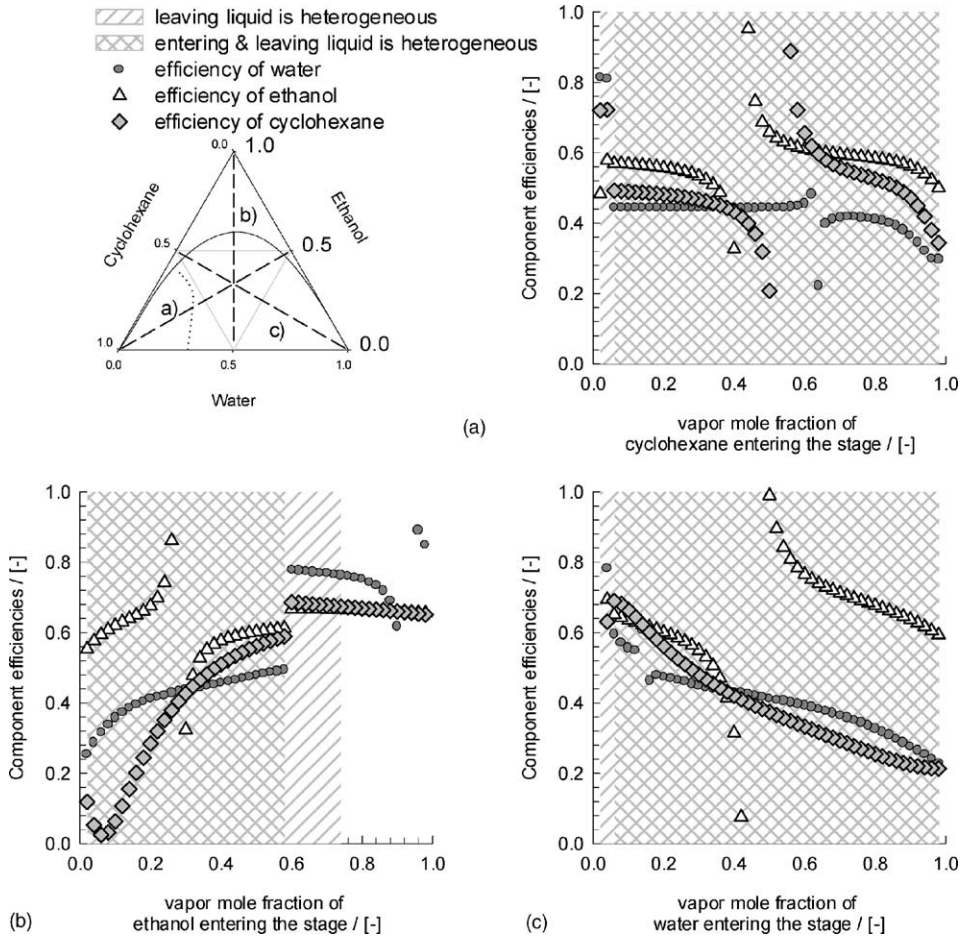

Fig. 7. Murphree component efficiencies for ethanol–water–cyclohexane system. The grey shaded region indicates the composition space wherein the liquid streams entering and leaving any particular stage are both heterogeneous.

the hurdle of the distillation boundary and bring the composition into the toluene rich region. The efficiency of water drops significantly as we move from stage 8 downward towards stages 10 and 11, where negative values are encountered. The negative efficiency of water serves to drive the composition trajectories away from the water rich region. The results shown in Fig. 6 demonstrate the very strong influence of liquid phase splitting on the component efficiencies.

7.2. Ethanol–water–cyclohexane system

Fig. 7a–c shows the component Murphree efficiencies for the ethanol–water–cyclohexane system along three different straight lines shown in the composition triangle in the top left part of Fig. 7. To construct this figure we have carried out calculations with a single-stage NEQ model. The composition of the vapor phase entering the stage was specified (at points along each line in the triangle) and total reflux operation was assumed. The bubble model was again used for estimating the mass transfer coefficients (bubble size 2.5 mm).

In all three cases we see that the efficiencies sometimes pass through an asymptotic discontinuity where the component efficiencies tend towards $\pm\infty$ due to the driving forces for mass transfer (composition differences) changing sign (Taylor & Krishna, 1993). This is the case for ethanol and water in all three illustrations and for cyclohexane in Fig. 7a. What is more striking, however, is the sudden jump discontinuity in the efficiencies shown in Fig. 7b as we move from the single liquid region to the two-liquid region. In this case there is a sudden change in the driving forces for mass transfer leading to the jump discontinuity in the efficiencies. The component efficiencies are much lower and more variable from component to component in the two-liquid phase region. In fact, the same behavior can be identified in Fig. 7a and c, but the simulations for these cuts were carried out almost totally in the heterogeneous liquid phase region, only a very small part of the composition space is in the single liquid phase region that lies close to the vertical axis in these figures. There is a much larger single liquid region for the cut shown in Fig. 7b.

We have carried out similar calculations over the entire composition triangle for this system leading to the Murphree efficiency maps shown in Fig. 8a–c. In general, we can see that the efficiencies are lower, sometimes significantly lower in the heterogeneous liquid region below the binodal curve. This fall off in efficiency is most obvious in Fig. 8a for water where we see efficiencies close to 100% in the single liquid phase region, falling to the 50–60% range just below

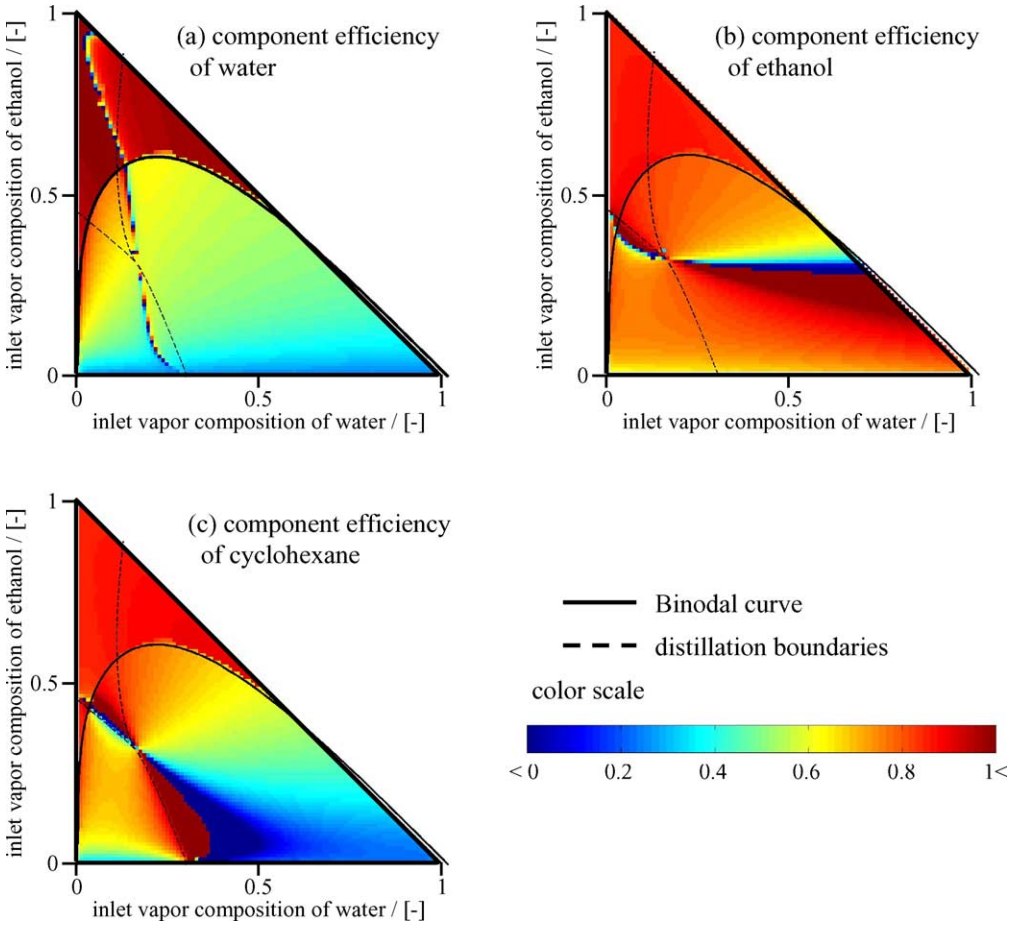

Fig. 8. Murphree component efficiency maps for (a) water; (b) ethanol; and (c) cyclohexane using the NEQ model.

the binodal curve, and all the way to 20% when the mole fraction of ethanol is very low. The efficiency of ethanol (Fig. 8b) is quite high almost everywhere, with the exception of a modestly sized part of the two-liquid phase region. The efficiency of cyclohexane (Fig. 8c) is high (80–90%) in the single-phase region, but there are large regions in the heterogeneous liquid phase region where the efficiency drops to 50% and sometimes is of the order of 20% or less. Fig. 8b and c both show a transition from a region with efficiencies that are close to unity (dark brown) to efficiencies that are close to zero (dark blue). The thick broken lines in Fig. 8 are the distillation boundaries.

8. Conclusion

A nonequilibrium model for a complete three-phase distillation process has been developed. The model consists of a set of mass and energy balances for each of the three possible phases present. Mass and heat transfer between these phases is described explicitly by means of the Maxwell–Stefan equations. Equilibrium is only assumed at the phase boundary between two phases. In the most general case, no mass transfer resistances are neglected. The equilibrium stage model is a special case of the general model. Incorporated into the model is a liquid phase stability check and phase split calculation to evaluate the thermodynamic stability of all liquid phases present in the distillation column each iteration.

Springer et al. (2003) have already demonstrated the NEQ model and method of solution described above works. The results of the nonequilibrium model were compared with experimental data obtained from a small laboratory scale column for the system water–ethanol–cyclohexane. In general a good match between numerical data and experiments was obtained. Mass transfer coefficients are obtained from a single-bubble mass transfer model, in which the only degree of freedom is the bubble diameter (that can be determined from binary distillation data if desired).

The method of solving the NEQ model equations described here consists of first solving the equilibrium two phase model, using this solution to obtain a converged solution for the equilibrium three-phase problem by means of a differential arc length continuation method, and subsequently using this as a starting guess for the nonequilibrium three-phase model, with an unconstrained Newton's method.

We have shown using NEQ model simulations that the component Murphree efficiencies tend to be lower and more highly variable in the two-liquid phase region than they are in the single liquid region. There may be a jump discontinuity in component efficiencies as we move from homogeneous to heterogeneous liquid phase regions of composition space. Differences in component efficiencies can lead to distillation products quite different from what would be anticipated on the basis of an equilibrium stage model. NEQ models for three-phase systems now exist and have been shown to be superior to EQ stage models at representing phenomena that actually do take place in such columns (e.g. crossing of the distillation boundaries predicted by an equilibrium model). This result lends further support to the recommendation that EQ models modified by efficiency factors should not, in general, be used for the simulation of three-phase distillation processes. NEQ models should be preferred in general. However, more work (largely experimental) is needed to develop generally applicable correlations of various parameters that are important for these models, for example, bubble sizes, froth heights, pressure drop.

References

Baden, N., & Michelsen, M. L. (1988). Computer methods for steady-state simulation of distillation columns. *Institution of Chemical Engineers Symposium Series, 104*, A425–A436.

Biegler, L. T., Grossmann, I. E., & Westerberg, A. W. (1997). *Systematic Methods of Chemical Process Design*. Upper Saddle River, NJ: Prentice Hall.

Block, U., & Hegner, B. (1976). Development and application of a simulation model for three-phase distillation. *American Institute of Chemical Engineers Journal, 22*, 582–589.

Cairns, B. P., & Furzer, I. A. (1990a). Multicomponent 3-phase azeotropic distillation. 1. Extensive experimental-data and simulation results. *Industrial & Engineering Chemistry Research, 29*, 1349–1363.

Cairns, B. P., & Furzer, I. A. (1990b). Multicomponent 3-phase azeotropic distillation. 2. Phase-stability and phase-splitting algorithms. *Industrial & Engineering Chemistry Research, 29*, 1364–1382.

Cairns, B. P., & Furzer, I. A. (1990c). Multicomponent 3-phase azeotropic distillation. 3. Modern thermodynamic models and multiple solutions. *Industrial & Engineering Chemistry Research, 29*, 1383–1395.

Davies, B., Ali, Z., & Porter, K. E. (1987). Distillation of systems containing two liquid phases. *American Institute of Chemical Engineers Journal, 33*, 161–163.

Doherty, M. F., & Malone, M. F. (2001). *Conceptual design of distillation systems*. New York: McGraw-Hill.

Eckert, E., & Vanek, T. (2001). Some aspects of rate-based modelling and simulation of three-phase distillation columns. *Computers & Chemical Engineering, 25*, 603–612.

Ferraris, G. B., & Morbidelli, M. (1981). Distillation models for two partially immiscible liquids. *American Institute of Chemical Engineers Journal, 27*, 881–888.

Ferraris, G. B., & Morbidelli, M. (1982). An approximate mathematical model for three-phase multistaged separators. *American Institute of Chemical Engineers Journal, 28*, 49–55.

Grohse, E. W., McCartney, R. F., Hauer, H. J., Gerster, J. A., & Colburn, A. P. (1949). Plate efficiencies in separation of C4 hydrocarbons by extractive distillation with furfural. *Chemical Engineering Progress, 45*, 725–738.

Higler, A., Krishna, R., & Taylor, R. (1999). Nonequilibrium cell model for multicomponent (reactive) separation processes. *American Institute of Chemical Engineers Journal, 45*, 2357–2370.

Kooijman, H. A. (1995). Dynamic nonequilibrium column simulations. Ph.D. dissertation, Clarkson University, Potsdam, New York.

Kooijman, H. A., & Taylor, R. (2001). *The ChemSep book*. Norderstedt, Germany: Books on Demand.

Kovach, J. W., & Seider, W. D. (1987). Heterogeneous azeotropic distillation homotopy-continuation methods. *Computers & Chemical Engineering, 11*, 593–605.

Krishna, R., & Wesselingh, J. A. (1997). The Maxwell–Stefan approach to mass transfer. *Chemical Engineering Science, 52*, 861–911.

Krishnamurthy, R., & Taylor, R. (1985). A nonequilibrium stage model of multicomponent separation processes. Part I. Model description and method of solution. *American Institute of Chemical Engineers Journal, 31*, 449–456.

Lao, M. Z., & Taylor, R. (1994). Modeling mass-transfer in 3-phase distillation. *Industrial & Engineering Chemistry Research, 33*, 2637–2650.

Lockett, M. J. (1986). *Distillation tray fundamentals*. Cambridge: Cambridge University Press.

Mendelson, H. D. (1967). The prediction of bubble terminal velocities from wave theory. *American Institute of Chemical Engineers Journal, 13*, 250–253.

Michelsen, M. L. (1982a). The isothermal flash problem. Part I. Stability. *Fluid Phase Equilibria, 9*, 1–19.

Michelsen, M. L. (1982b). The isothermal flash problem. Part II. Phase-split calculation. *Fluid Phase Equilibria, 9*, 21–40.

Mortaheb, H. R., Kosuge, H., & Asano, K. (2002). Hydrodynamics and mass transfer in heterogeneous distillation with sieve tray column. *Chemical Engineering Journal, 88*, 59–69.

Poling, B. E., Prausnitz, J. M., & O'Connell, J. P. (2001). *The properties of gases and liquids* (5th ed.). New York: McGraw-Hill.

Prokopakis, G. J., Seider, W. D., & Ross, B. A. (1981). Azeotropic distillation towers with two liquid phases. In *Proceedings of the Interantional Conference on the Foundation of Computer-Aided Chemical Process and Design* (vol. 2, pp. 239–272).

Repke, J. -U., & Wozny, G. (2001). A nonequilibrium model for three-phase distillation in a packed column. In *Proceedings Volume from the IFAC Symposium on Advanced Control of Chemical Processes* (vol. 3, pp. 995–1000). Pisa, Italy, 14–16 June 2000.

Repke, J. U., & Wozny, G. (2002). Experimental investigations of three-phase distillation in a packed column. *Chemical Engineering & Technology, 25*, 513–519.

Ross, B. A., & Seider, W. D. (1981). Simulation of three-phase distillation towers. *Computers & Chemical Engineering, 5*, 7–20.

Schoenborn, E. M., Koffolt, J. H., & Withrow, J. R. (1941). Rectification in the presence of an insoluble component. *Transactions of the American Institute of Chemical Engineers, 37*, 997–1021.

Schuil, J. A., & Bool, K. K. (1985). Three-phase flash and distillation. *Computers & Chemical Engineering, 9*, 295–300.

Seader, J. D. (1985). The B.C. (before computers) and A.D. of equilibrium-stage operations. *Chemical Engineering Education, 19*(2), 88–103.

Seader, J. D., & Henley, E. J. (1998). *Separation process principles*. New York: Wiley.

Smith, J. V., Missen, R. W., & Smith, W. R. (1993). General optimality criteria for multiphase multireaction chemical-equilibrium. *American Institute of Chemical Engineers Journal, 39*, 707–710.

Springer, P. A. M., Baur, R., & Krishna, R. (2003). Composition trajectories for heterogeneous azeotropic distillation in a bubble-cap tray column: Influence of mass transfer. *Chemical Engineering Research & Design, 81*, 413–426.

Swartz, C. L. E., & Stewart, W. E. (1987). Finite-element steady state simulation of multiphase distillation. *American Institute of Chemical Engineers Journal, 33*, 1977–1985.

Taylor, R., & Krishna, R. (1993). *Multicomponent mass transfer*. New York: Wiley.

Taylor, R., Krishna, R., & Kooijman, H. (2003). Real-world modeling of distillation. *Chemical Engineering Progress, 98*(7), 28–39.

Wesselingh, J. A., & Krishna, R. (2000). *Mass transfer in multicomponent mixtures*. Delft: Delft University Press.

Westerberg, A. W., Hutchison, H. P., Motard, R. L., & Winter, P. (1979). *Process flowsheeting*. Cambridge, UK: Cambridge University Press.

Woodman, M. W. (1989). Simulation of the distillation of three phase mixtures. Ph.D. dissertation, Cambridge University, Cambridge, UK.